Original Article

Analysis of left anterior segmental bronchovascular patterns and its benefits for surgical implications: a retrospective cross-sectional study

Tao Long[1#^], Junqing Qi[1#], Aizhong Shao[1#], Jingfeng Zhu[1], Huiwen Pan[1], Yijun Shi[1], Zhengbing Ren[1], Zhicheng He[2], Weibing Wu[2]

[1]Department of Cardiothoracic Surgery, Affiliated People's Hospital of Jiangsu University, Zhenjiang, China; [2]Department of Thoracic Surgery, The First Affiliated Hospital of Nanjing Medical University, Nanjing, China

Contributions: (I) Conception and design: T Long, W Wu; (II) Administrative support: W Wu, Z Ren; (III) Provision of study materials or patients: Z He, W Wu; (IV) Collection and assembly of data: T Long, J Qi, A Shao; (V) Data analysis and interpretation: T Long, J Zhu, H Pan, Y Shi; (VI) Manuscript writing: All authors; (VII) Final approval of manuscript: All authors.

[#]These authors contributed equally to this work.

Correspondence to: Weibing Wu, MD. Department of Thoracic Surgery, The First Affiliated Hospital of Nanjing Medical University, No. 300 Guangzhou Road, Gulou District, Nanjing 210029, China. Email: wuweibing95@163.com.

Background: Sublobar surgeries involving the left anterior segment of the lung can be challenging due to its central location within the left upper lobe (LUL) and among multi-segments. However, there have been no reports specifically analysing the anatomical patterns of this segment. Therefore, this study aimed to comprehensively investigate the subsegmental bronchovascular patterns and relationship between variations and surgical strategies.

Methods: The branching patterns of the left anterior segment bronchi and pulmonary vessels were assessed retrospectively and categorised using three-dimensional reconstruction images of 647 consecutive patients.

Results: Anatomical distribution patterns of the left anterior segmental bronchus, artery, and vein analysed in 635 valid cases were 6, 38, and 6, respectively. For the first time, branches of the sub-subsegmental level were demonstrated and reclassified in the anterior segment. Additionally, all 102 cases (16.06%) of interlobar (IL) arterial variations were found in the lateral subsegmental artery. Interestingly, only the lateral subsegmental artery patterns were not independent of the types associated with the anterior segmental bronchus, artery, and vein in the left upper division. Based on the observed anatomical variant patterns of the artery and bronchus, we developed a decision-making theory to assist in selecting surgical approaches for nodules located within the lateral subsegment of the anterior segment of the lung.

Conclusions: The study elucidated the sub-subsegmental level of the left anterior segmental bronchovascular distribution patterns. This study also indicated a correlation between the lateral subsegmental arterial patterns and the patterns observed in the anterior bronchus and the left upper division vein (LUDV). By taking these findings on arterial and bronchial variations into account preoperatively, we might contribute to formulating a more concise operation procedure and optimizing the selection of surgical approaches.

Keywords: Left anterior segmental anatomic variation; pulmonary nodules; decision theory tree; three-dimensional computed tomography bronchography and angiography (3-D CTBA)

Submitted Aug 26, 2024. Accepted for publication Dec 05, 2024. Published online Jan 22, 2025.
doi: 10.21037/jtd-24-1397
View this article at: https://dx.doi.org/10.21037/jtd-24-1397

^ ORCID: 0000-0002-2347-2807.

Introduction

Recent landmark clinical studies, including the JCOG0802 (1) and CALGB140503 (2) trials, have demonstrated the efficacy of sub-lobar resections for tumours smaller than 2 cm and for clinical stage T1aN0 non-small cell lung cancer with ground-glass opacity components. Sublobar resections can be categorised into wedge resections, segmentectomies, and subsegmentectomies. Nowadays, the anatomic precise segmentectomies encompass a wide spectrum, varying from the resection of a single segment or subsegment to the combined resections of multiple segments or subsegments. Therefore, the surgical procedure relies heavily on a comprehensive understanding of the subsegmental anatomy of the lung.

Unlike traditional anatomy on cadavers, three-dimensional computed tomography bronchography and angiography (3-D CTBA) offer a non-invasive approach to understanding the complex organization of lung anatomy and indicate the significance of understanding these variations in surgical planning even when using only noncontrast computed tomography (CT) data. As one of the automated noncontrast CT reconstruction algorithm software, InferOperate Thoracic Surgery (3) has been widely accepted for its higher accuracy and automation.

The left upper lobe (LUL) has a higher prevalence of anatomical variations and severe complications (4). Within this lobe, the left anterior segment (LS^3) lateral subsegment is located centrally at the junction of multiple subsegments, rendering surgical procedures in this area particularly challenging.

The watershed analysis (5) method has demonstrated its feasibility for wedge resections by temporarily blocking specific arteries. Moreover, another study (6) has reported that after splitting the left upper division and lingular, combined subsegmentectomy containing LS^3 can be possible and safe. However, existing studies have not thoroughly investigated the variations in LS^3.

Given the lack of comprehensive research on anatomical variations in this specific region, a comprehensive investigation is necessary to clarify the LS^3 subsegmental bronchi and vessel patterns. For complex nodules located in the lateral subsegment of left anterior segment (LS^3a), efficiently understanding and utilising these anatomical variations remains unresolved. To solve those problems, our study focuses on the distribution of LS^3 bronchovascular patterns, particularly the incidence rate of an interlobar (IL) left anterior artery (A^3), which has not been previously reported. We also hypothesize that preoperatively finding the anatomical variations may concise the operation and optimise the selection of the surgical approach for pulmonary nodules located in the LS^3a. We present this article in accordance with the STROBE reporting checklist (available at https://jtd.amegroups.com/article/view/10.21037/jtd-24-1397/rc).

Highlight box

Key findings

- We clarified the detailed bronchovascular distribution within the left anterior segment from the level of sub-subsegmental branch and explored its advantages in surgical approaches selection.

What is known and what is new?

- Subsegmental bronchovascular variations are already well-documented.
- Sub-subsegmental level bronchovascular patterns of left anterior segment are newly discovered and reclassified in our study. For the first time, we summarized a novel decision tree for selecting surgical approaches for nodules located within the S^3a by exploiting the anatomical variations.

What is the implication, and what should change now?

- The study suggests that the abnormal interlobar A^3a is significant in determining the selection of surgical methods.
- It is recommended to pay more attention to variations in A^3a before surgery by utilizing three-dimensional computed tomography bronchography and angiography to optimize the surgical approach accordingly.

Methods

Patients and 3-D CTBA

This retrospectively cross-sectional study enrolled 647 consecutive hospitalised patients who underwent thoracoscopic surgeries because of pulmonary nodules between March 2023 and August 2023 in the Thoracic Surgery Department of The First Affiliated Hospital of Nanjing Medical University. Subsequently, raw data from their CT scan were collected for reconstruction. 3-D CTBA models of patients were automatically processed and manually analysed using the InferOperate Thoracic Surgery software based on chest CT data. After excluding six cases due to malformation and another six cases for having surgical histories of LUL, 635 available cases (329 women and 306 men) were finally included, having a mean age of 50.1 years (range, 24–79 years). To control information bias, one surgeon underwent systematic training about the

anatomical naming rules of the pulmonary system. After completing the training, the surgeon conducted systematic training and assessment for another two colleagues. Subsequently, three experienced thoracic surgeons confirmed the validity of all models. If different opinions arose, the final decision was made after discussion. Finally, distribution patterns of LS^3 bronchus, arteries, and left upper division veins (LUDVs) were collected to classify and summarise. The nomenclature systems are illustrated below.

Inclusion criteria

(I) Chest CT exams with a slice thickness ≤1.5 mm, including non-contrast and contrast-enhanced CT scans.
(II) Availability of 3-D models of LUL bronchi and vessels.
(III) No previous history of left upper lung surgery.

Exclusion criteria

(I) Chest CT thickness exams over 1.5 mm.
(II) A history of left upper lung surgery.
(III) Dispute among experts regarding the validity of the reconstruction models.

Ethical statement

The study was conducted in accordance with the Declaration of Helsinki (as revised in 2013). The study was approved by the Ethics Committee of Affiliated People's Hospital of Jiangsu University (No. SQK-20220166-Y) and individual consent for this retrospective analysis was waived.

Definition of left upper lobar bronchi (B), arteries (A), and veins (V)

According to the nomenclature systems of Boyden (7), Yamashita (8), and the textbook of Chen *et al.* (9), the left apicoposterior segment (S^{1+2}) is composed of apical (S^{1+2}a), posterior (S^{1+2}b), and lateral (S^{1+2}c). The left anterior segment could be classified into lateral (S^3a), medial (S^3b), and superior (S^3c) subsegments. Correspondingly, the bronchial names were labelled as B^{1+2}a, b, and c and B^3a, b, and c, while the arterial names were labelled as A^{1+2}a, A^{1+2}b, A^{1+2}c, A^3a, A^3b, and A^3c. According to Boyden (7), the first priority principle is superior and inferior, the second priority principle is posterior and anterior, and the last priority principle is lateral and internal. Sub-subsegments were designated with Roman numerals (i, ii, and iii), while the sub-subsegments were designated in the Greek alphabet (α, β, and γ). The apicoposterior segment vein (V^{1+2}) consisted of four branches: V^{1+2}a, V^{1+2}b, V^{1+2}c, and V^{1+2}d, although it may have a branch Vl. The anterior segment vein (V^3) consisted of three branches: V^3a, V^3b and V^3c. Normally, LUDV is comprised of three types: central vein, semi-central vein, and non-central vein.

Statistical analysis

All statistical analyses were conducted utilising Statistical Package for the Social Sciences software (version 27.0; Chicago, IL, USA). Descriptive data are summarised as the number of cases (%). We used the cross-tabulation method to analyse the correlations among the bronchus, artery, and vein. Fisher's exact test was employed to assess the significance of associations between groups because over 20% of the cells contained counts less than 5, and some contained minimum expected counts below 1. In this study, a $P<0.01$ was considered statistically significant.

Results

Left B^3 branching patterns

The left S^3 branching patterns are detailed in *Table 1*, and images illustrating these patterns are displayed in *Figure 1*. In a study of 635 patients, six types of bronchial bifurcation and one trifurcation type were identified. The most common bifurcation type was B^3a, B^3b+c, found in 471 patients (74.17%). Meanwhile, there was only one instance of B^3a, B^3b+c belonging to left eparterial bronchus (11). Conversely, B^3a+b, B^3c, B^3a+c, and B^3b patterns were observed in 85 (13.39%) and 1 (0.16%), respectively. Interestingly, B^3ai, B^3aii+b+c type was reported for the first time in 17 (2.68%) patients. The BX^3a, B^3b+c type exhibited a descending pattern of B^3a, potentially arising from the main trunk part of the left upper division bronchus either alone (4, 0.63%) or with B^{1+2}c (2, 0.31%). The trifurcation type B^3a, B^3b, and B^3c was observed in 55 patients (8.66%).

Left A^3 branching patterns

This study represented the first anatomic distribution of the level of sub-sub-subsegmental pulmonary arteries, indicating that conventional classification systems are not

Table 1 Branching patterns of left upper division bronchus

Bronchial type	Subtype	Displacement of X	Figure location	Our study (N=635)	Li *et al.* (10) (N=540)
Bifurcated				580 (91.34)	
	B^3a+b, B^3c		*Figure 1A*	85 (13.39)	70 (13.0)
	B^3a, B^3b+c		*Figure 1B*	470 (74.02)	373 (69.0)
	B^3a+c, B^3b		*Figure 1C*	1 (0.16)	NR
	$BX^3a^{\dagger}$, B^3b+c				NR
		With $B^{1+2}c$	*Figure 1D*	2 (0.31)	NR
		B^3a Singly	*Figure 1E*	4 (0.63)	NR
	B^3ai, B^3aii+b+c		*Figure 1F*	17 (2.68)	NR
	B^3a, B^3b+c (left eparterial bronchus‡)		*Figure 1G*	1 (0.16)	2 (0.4)
Trifurcated				55 (8.66)	
	B^3a, B^3b, B^3c		*Figure 1H*	55 (8.66)	95 (17.6)

Data are presented as n (%). †, descending of B^3a to the trunk of left upper division; ‡, special type of B^3a, B^3b+c with abnormal. X, mean abnormal origin; B, bronchus; ^{3}, anterior segment; ^3a, lateral subsegment; ^3b, medial subsegment; ^3c, superior subsegment; characters i and ii means sub-subsegmental branches; NR, no record.

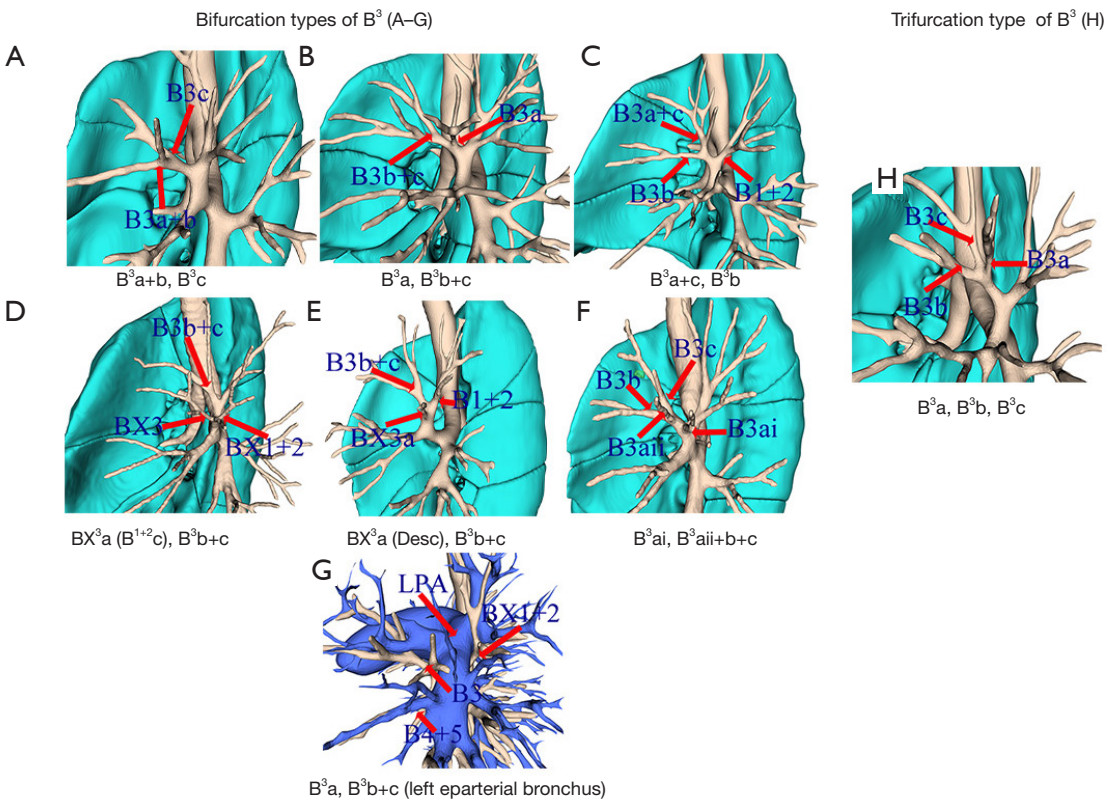

Figure 1 Images of eight left anterior segmental bronchus (B^3) branching patterns. (A) B^3a+b, B^3c; (B) B^3a, B^3b+c; (C) B^3a+c, B^3b; (D) BX^3a ($B^{1+2}c$), B^3b+c; (E) BX^3a (Desc), B^3b+c; (F) B^3ai, B^3aii+b+c; (G) B^3a, B^3b+c (left eparterial bronchus); (H) B^3a, B^3b, B^3c. X, mean abnormal origin; B, bronchus; ^{3}, anterior segment; ^3a, lateral subsegment; ^3b, medial subsegment; ^3c, superior subsegment; $^{1+2}$, apicoposterior segment; ^{4}, superior lingular segment; ^{5}, inferior lingular segment; LPA, left pulmonary artery; Desc, descending of B^3a to the trunk of left upper division; characters "i", "ii" mean sub-subsegmental branches.

Table 2 Simplified branching patterns of left anterior segmental artery (A^3)

A^3 branches	Types	Origins						No. (%)
		LPA	A^{1+2}a+b	MLA	IL-LPA	IL-A^{1+2}c	LA	
One	Type 1	√						463 (72.91)
Two								164 (25.83)
	Type 2	√						36 (5.67)
	Type 3	√	√					9 (1.42)
	Type 4	√		√				23 (3.62)
	Type 5		√	√				1 (0.16)
	Type 6	√			√			33 (5.2)
	Type 7	√				√		15 (2.36)
	Type 8	√					√	47 (7.4)
Three								8 (1.26)
	Type 9	√		√				1 (0.16)
	Type 10	√		√	√			3 (0.47)
	Type 11	√			√		√	2 (0.31)
	Type 12	√				√		1 (0.16)
	Type 13	√			√			1 (0.16)
Total		634 (99.84)	10 (1.57)	28 (4.41)	39 (6.14)	16 (2.52)	49 (7.72)	

A, artery; ^{3}, anterior segment; LPA, left pulmonary artery; $^{1+2}$, apicoposterior segment; MLA, mediastinal lingular artery; IL, interlobar; LA, lingular artery; $^{1+2}$a, apical subsegment; $^{1+2}$b, posterior subsegment; $^{1+2}$c, lateral subsegment.

applicable. We summarised 13 types based on the number of branches, the presence of IL arteries, and six different sources of arterial origin from 38 subtypes, as detailed in *Table 2* and Table S1. Additionally, *Figures 2*,*3* are the detailed images of these findings. In one branch type, only the mediastinal (M) type 1 was found in 463 patients (72.91%). The IL type that was reported (10) previously was not observed. While in the 164 cases (25.83%) of the two branch groups, type 2 comprised 36 cases that arose from the proximal left pulmonary artery (LPA). Apart from these two types, all other identified types displayed abnormal origins, which are detailed in *Table 2*. There were 8 cases (1.26%) that consisted of three A^3 branches. Moreover, 28 cases (4.41%) exhibited abnormal branches originating from the mediastinal lingular artery (MLA). All 102 mediastinal and interlobar (MIL) type cases (16.06%) exhibited anatomic variations involving AX^3a and its ramus.

Left A^3a branching patterns

As detailed in *Table 3*, the A^3a branching patterns consisted of single (560, 88.19%), double (74, 11.65%), and triple (1, 0.16%) patterns. The specifics are provided in Table S2. More specifics are listed in Table S2, including the same pictures as A^3 and location information in column 5 of Table S2. The IL pulmonary artery (55, 8.66%) and lingular artery (LA) (49, 7.72%) represented the two most common abnormal origins types. The IL pulmonary artery consisted of two sub-types, including 39 cases (6.14%) originating from the IL portion of LPA singly or 16 cases (2.52%) sharing the same trunk with A^{1+2}c originating from LPA. Another two types, ectopic origins, accounted for 9 cases (1.42%) in A^{1+2}a+b and 14 cases (2.20%) in MLA, respectively. Moreover, the total incidence rate of sub-subsegmental arteries and its ramus was 11.7% (74/635).

Left upper division venous branching patterns

According to the nomenclature by Yamashita (8) and Wang *et al.* (12) regarding the left upper division venous pattern, the distribution of semi-central vein type (413, 65.04%), central vein type (178, 28.03%), and non-central vein type

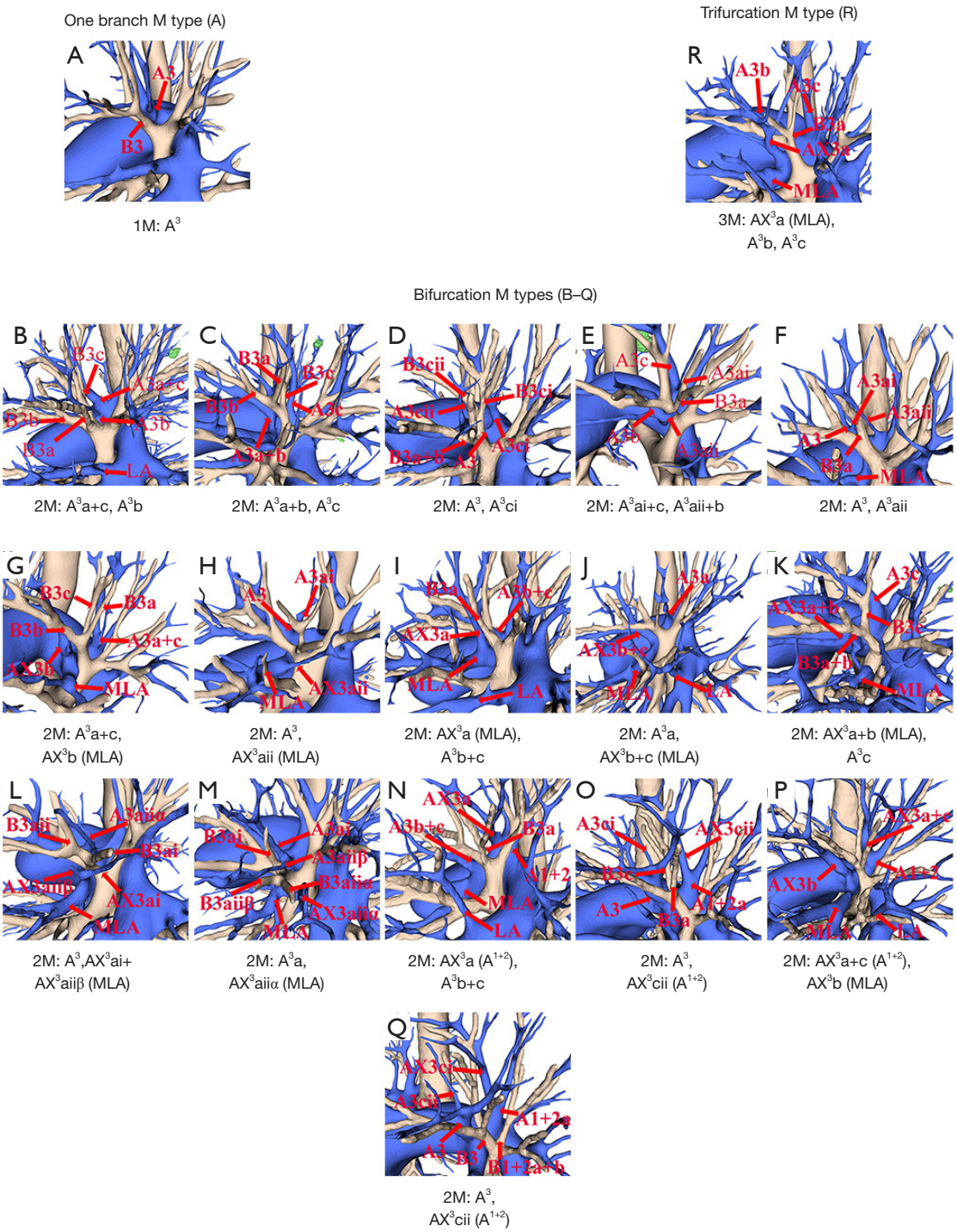

Figure 2 Images of 18 M types of left segmental artery. (A) A^3; (B) A^3a+c, A^3b; (C) A^3a+b, A^3c; (D) A^3, A^3ci; (E) A^3aii+b, A^3ai+c; (F) A^3, A^3aii; (G) A^3a+c, AX^3b; (H) A^3, AX^3aii; (I) AX^3a, A^3b+c; (J) A^3a, AX^3b+c; (K) AX^3a+b, A^3c; (L) A^3, AX^3ai+AX^3aiiβ; (M) A^3, AX^3aiiα; (N) AX^3a, A^3b+c; (O) A^3, AX^3ci; (P) A^3, AX^3cii; (Q) AX^3a+c, AX^3b; (R) AX^3a, A^3b, A^3c. A, artery; ^{3}, anterior segment; 1, one branch; M, mediastinal; 2, two branches; 3, three branches; $^{1+2}$, apicoposterior segment; LA, lingular artery; MLA, mediastinal lingular artery; ^{3}, anterior segment; X, mean abnormal origin; ^{3}a, lateral subsegment; ^{3}b, medial subsegment; ^{3}c, superior subsegment; characters "i", "ii", "iii" mean sub-subsegmental branches; characters "α", "β" mean sub-sub-subsegmental branch.

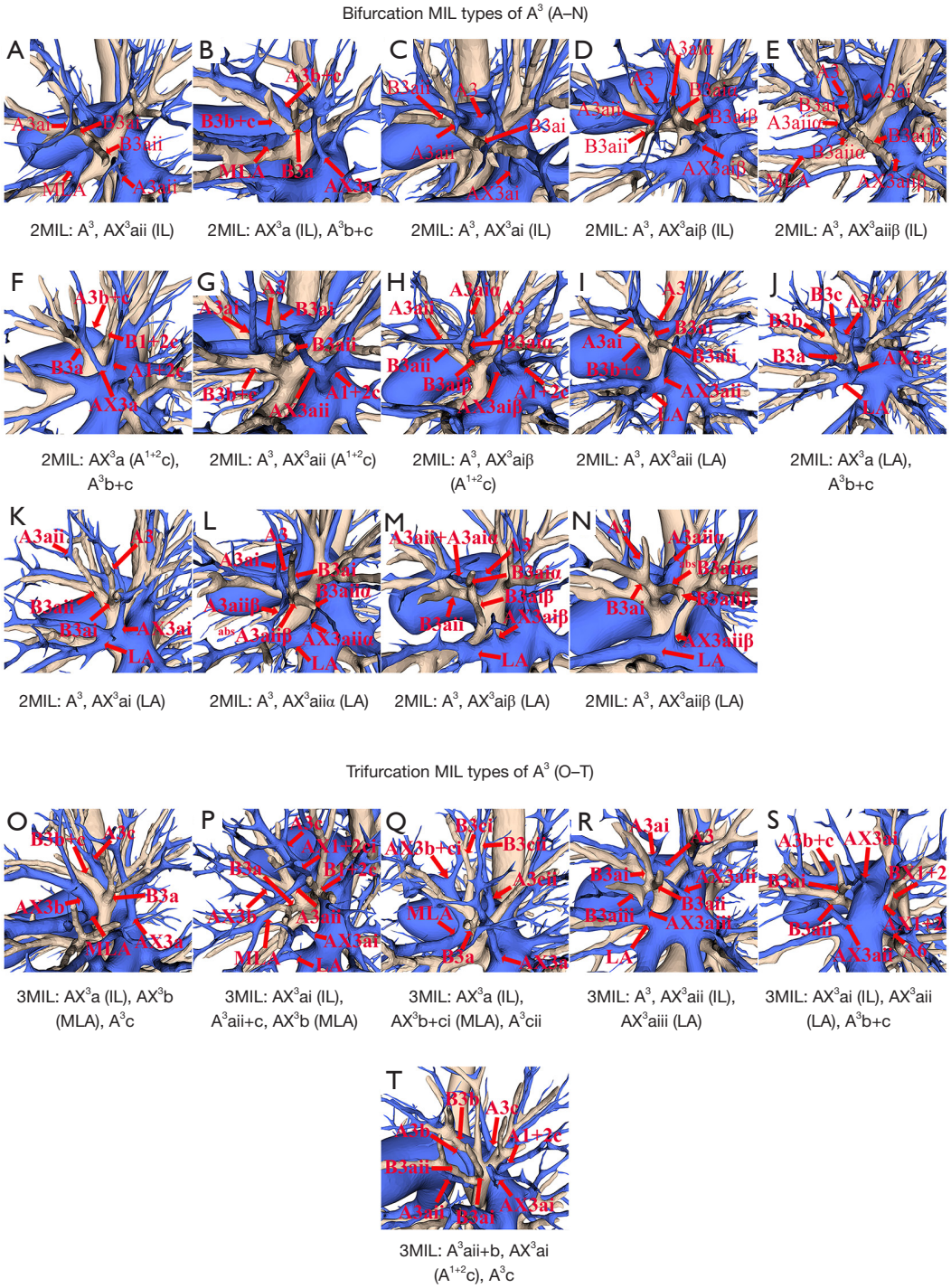

Figure 3 Images of 20 MIL types of A³. (A) A³, AX³aii (IL); (B) AX³a (IL), A³b+c; (C) A³, AX³ai (IL); (D) A³, AX³aiβ (IL); (E) A³, AX³aiiβ (IL); (F) AX³a (A¹⁺²c), A³b+c; (G) A³, AX³aii (A¹⁺²c); (H) A³, AX³aiβ (A¹⁺²c); (I) A³, AX³aii (LA); (J) AX³a (LA), A³b+c; (K) A³, AX³ai (LA); (L) A³, AX³aiiα (LA); (M) A³, AX³aiβ (LA); (N) A³, AX³aiiβ (LA); (O) AX³a (IL), AX³b (MLA), A³c; (P) AX³ai (IL), A³aii+c, AX³b (MLA); (Q) AX³a (IL), AX³b+ci (MLA), A³cii; (R) A³, AX³aii (IL), AX³aiii (LA); (S) AX³ai (IL), AX³aii (LA), A³b+c; (T) A³aii+b, AX³ai (A¹⁺²c), A³c. A, artery; ³, anterior segment; 2, two branches of A³; MIL, mediastinal and interlobar; 3, three branches of A³; ¹⁺², apicoposterior segment; MLA, mediastinal lingular artery; IL, interlobar; LA, lingular artery; X, mean abnormal origin; ³a, lateral subsegment; ³b, medial subsegment; ³c, superior subsegment; characters "i", "ii", "iii" mean sub-subsegmental branches; characters "α", "β" mean sub-sub-subsegmental branch.

Table 3 Simplified 13 branching patterns of the lateral subsegment of left anterior segmental artery (A^3a)

A^3a branches	Types	Origins						No. (%)
		A^3 and LPA	$A^{1+2}a+b$	MLA	IL-LPA	IL-$A^{1+2}c$	LA	
One								560 (88.19)
	Type I	√						505 (79.53)
	Type II		√					9 (1.42)
	Type III			√				6 (0.94)
	Type IV				√			16 (2.52)
	Type V					√		9 (1.42)
	Type VI						√	15 (2.36)
Two								74 (11.65)
	Type VII	√						5 (0.79)
	Type VIII	√		√				8 (1.26)
	Type IX	√			√			21 (3.31)
	Type X	√				√		7 (1.10)
	Type XI	√					√	32 (5.04)
	Type XII				√		√	1 (0.16)
Three								1 (0.16)
	Type XIII	√			√		√	1 (0.16)
Total		579 (91.18)	9 (1.42)	14 (2.20)	39 (6.14)	16 (2.52)	49 (7.72)	

A, artery; ^{3}a, lateral subsegment; ^{3}, anterior segment; LPA, left pulmonary artery; $^{1+2}$, apicoposterior segment; MLA, mediastinal lingular artery; IL, interlobar; LA, lingular artery; $^{1+2}$a, apical subsegment; $^{1+2}$b, posterior subsegment; $^{1+2}$c, lateral subsegment.

(44, 6.92%) are outlined in *Table 4* and *Figure 4*. In addition to the five known types, we identified a rare new type named non-central O type, observed in two cases where $V^{1+2}c$ abnormally drains blood to V^6. Similarly, the semi-central A type was the most common, accounting for nearly half the total (317, 49.92%).

Correlation analysis of A^3a patterns, bronchus patterns, and venous patterns

Our statistics revealed that A^3, A^3a, and B^3a and venous patterns of the left upper division comprised 38, 26, 7, and 6 different types, respectively. However, there are likely even more variations. Based on our clinical experience, we optimised these patterns. The classifications are detailed in *Tables 1-4*. The number of arterial branches and their original types were analysed independently. We analysed the correlations among all bronchovascular patterns. Significant relationships (all $P<0.001$) were observed between A^3a branches number, origins, and subtype classification with A^3 patterns, B^3 patterns, and left upper division venous patterns, as outlined in *Table 5*.

Decision theory tree

According to the bronchovascular variation types of the left anterior segment, particularly the lateral subsegmental arteries and bronchus variants, we developed an anatomical variation-associated surgical decision tree for the ≤2 cm nodules located in the middle-lateral zone of the left lateral anterior subsegment. Our theory is illustrated in *Figure 5*. For subsegment A^3a, classified as M type, the primary surgical plan recommended was intra-venous single-direction approach surgery regardless of the bronchus type. If A^3a includes the IL ramus sharing the trunk with IL $A^{1+2}c$ along with the bronchus type $B^3a+B^{1+2}c$,

Table 4 Branching patterns of left upper division bronchus

Venous type	Veins variation	Our study (N=635)	Wang *et al.* (12) (N=805)
Central vein		178 (28.03)	207 (25.71)
Central-A type		147 (23.15)	175 (21.74)
Central-B type		31 (4.88)	32 (3.97)
Semi-central vein		413 (65.04)	504 (62.61)
Semi-central A type		317 (49.92)	418 (51.93)
Semi-central B type		96 (15.12)	86 (10.68)
Non-central vein		44 (6.92)	87 (10.81)
Non-central type		42 (6.61)	80 (9.94)
Non-central O type	V^{1+2}c drains blood to V^{6}‡	2 (0.31)	7 (0.87)

Data are presented as n (%). ‡, this type of variation only represents in our study. V^{1+2}c means intersubsegment vein between posterior subsegment of S^{1+2} and lateral subsegment of S^{1+2}c; V, vein; $^{1+2}$, apicoposterior segment; ^{6}, superior segment of lower lobe.

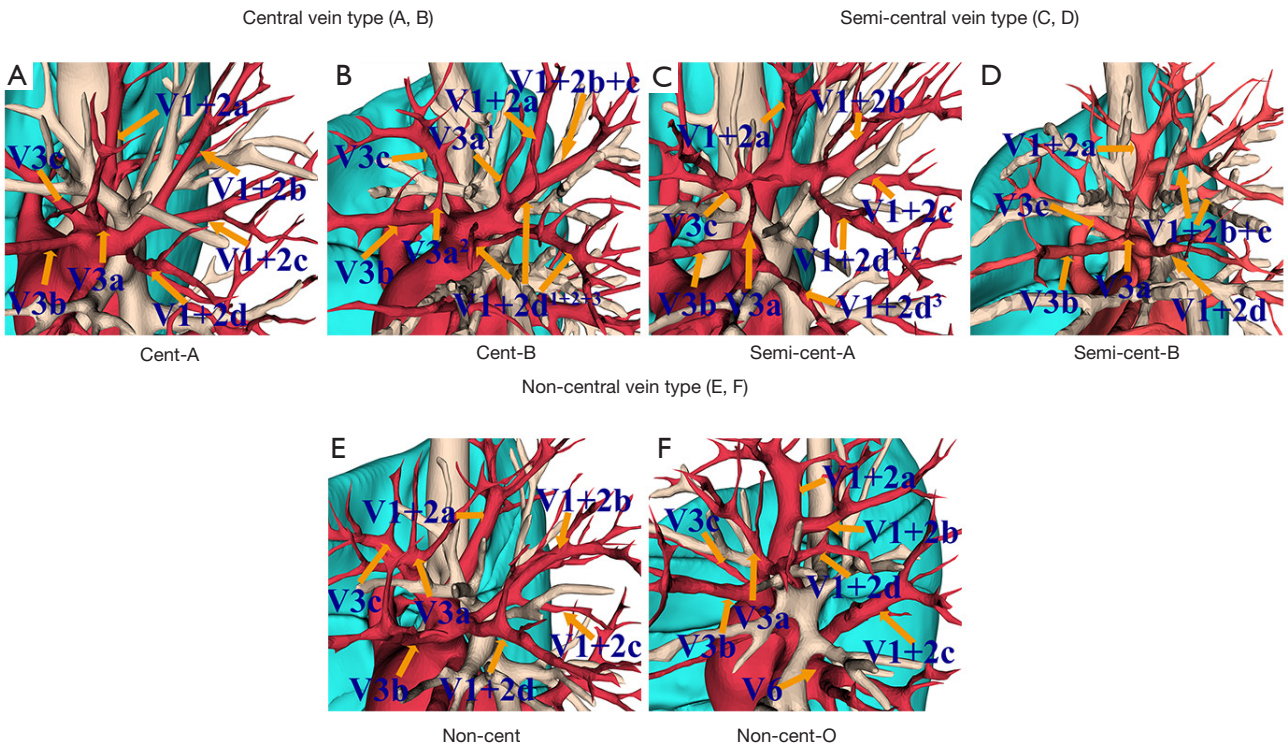

Figure 4 3-dimensional images of six left upper division venous branching patterns. (A) Cent-A; (B) Cent-B; (C) Semi-cent A; (D) Semi-cent B; (E) Non-cent; (F) Non-cent-O. V, vein; B, bronchus; S, segment; $^{1+2}$, apicoposterior segment; ^{3}, anterior segment; V^{1+2}a, intra-segmental vein between apical subsegment and superior subsegment of S^{3}; V^{1+2}b, intersubsegment vein between S^{1+2}a and S^{1+2}b; V^{1+2}c, intersubsegment vein between posterior subsegment of S^{1+2} and lateral subsegment of S^{1+2}c; V^{1+2}d, intersubsegment vein among lateral subsegment of S^{1+2} and lateral subsegment of S^{3} and lateral subsegment of superior lingular segment; V^{3}a, intersubsegment vein between lateral subsegment of S^{3} and superior subsegment of S^{3}, and between lateral subsegment of S^{3} and medial subsegment of S^{3}; V^{3}b, intersubsegment vein between medial subsegment of S^{3} and anterior subsegment of lingular; V^{3}c, intersubsegment vein between medial subsegment of S^{3} and superior subsegment of S^{3}; A, artery; $^{1+2}$c, lateral subsegment; 6, superior segment of the left lower lobe.

Table 5 Results of Fisher's exact test of A^3a branches, origins, and subtype and other bronchovascular types of left upper division

Detail types	P value		
	A^3a branches type	A^3a M-IL type	A^3a subtype
B^3 types	<0.001***	<0.001***	<0.001***
A^3 branches types	<0.001***	<0.001***	<0.001***
A^3 M-IL types	<0.001***	<0.001***	<0.001***
A^3 subtypes	<0.001***	<0.001***	<0.001***
Left upper division pulmonary vein types	<0.001***	<0.001***	<0.001***

***, significant at the 0.001 probability level. A, artery; B, bronchus; ^{3}, anterior segment; M, mediastinal; IL, interlobar; ^{3}a, lateral subsegment.

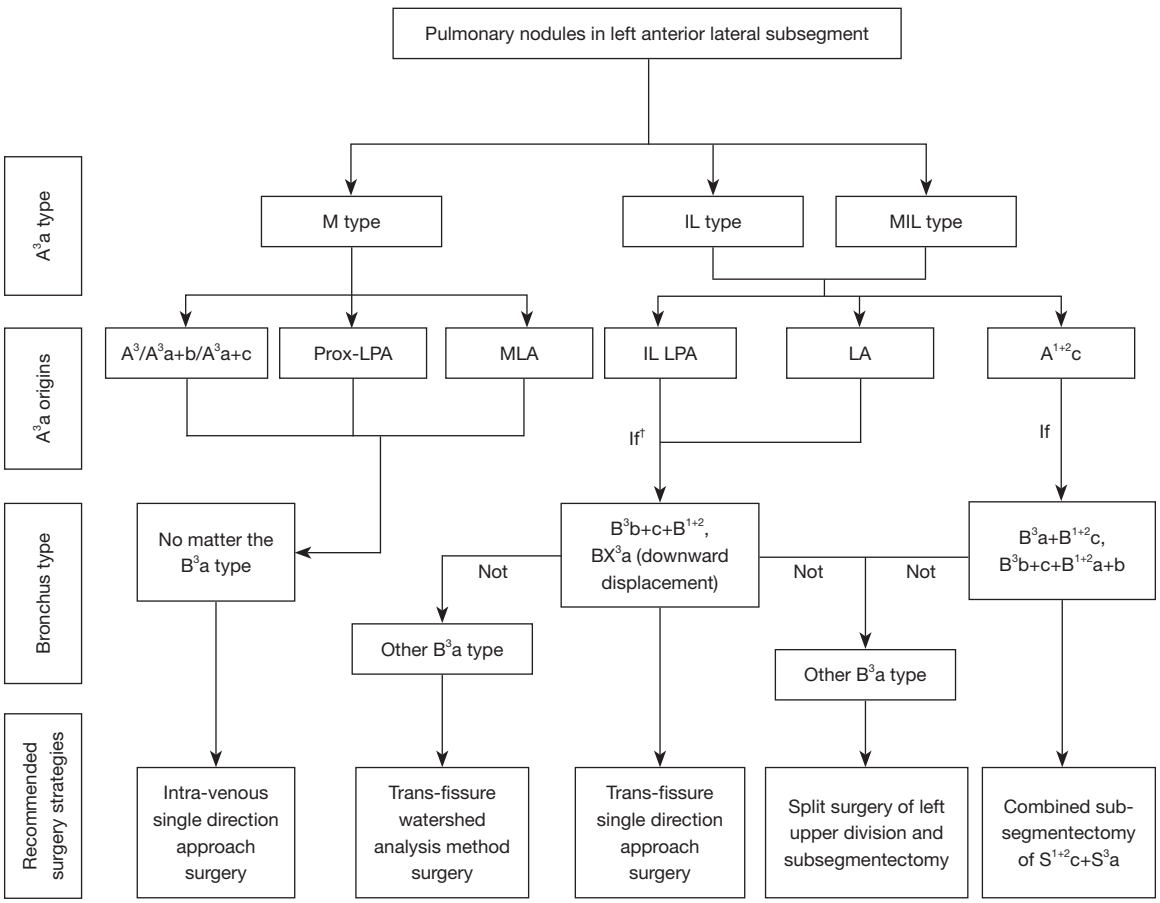

Figure 5 Decision theory tree of surgeries related lateral subsegment of LS^3a based on arterial and bronchial patterns. †, both the type of IL LPA and LA is OK. A, artery; M, mediastinal; IL, interlobar; MIL, mediastinal and interlobar; LPA, left pulmonary artery; $^{1+2}$, apicoposterior segment; MLA, mediastinal lingular artery; LA, lingular artery; B, bronchus; ^{3}, anterior segment; X, mean abnormal origin; $^{1+2}$a, apical subsegment; $^{1+2}$b, posterior subsegment; $^{1+2}$c, lateral subsegment; ^{3}a, lateral subsegment; ^{3}b, medial subsegment; ^{3}c, superior subsegment; S, segment.

$B^3b+c+B^{1+2}a+b$, combined subsegmentectomy of $S^{1+2}c+S^3a$ was recommended. Conversely, split surgery of the left upper division and S^3a subsegmentectomy were suggested. Moreover, trans-fissure single-direction approach surgery was recommended as an easier surgical procedure for single-branch IL A^3a and descending B^3a. Besides, there were two operation plans for IL A^3a type and MIL A^3a type. One plan was trans-fissure Watershed analysis method surgery, which simplifies the procedure and shortens operation time, while the other was split surgery of left upper division and S^3a subsegmentectomy for experienced surgeons.

Discussion

We conducted a comprehensive analysis of bronchovascular patterns using three-dimensional models of 635 patients, revealing new insights into the intricate relationship between these structures and the implications for surgical strategy. Our findings include identifying and reclassifying sub-subsegmental branches and the development of a decision tree to aid surgeons in surgical decision-making.

The current classification system of LUL pulmonary subsegments has predominantly relied on anatomical models developed by researchers such as Boyden (7) and Yamashita (8). As our comprehension of lung anatomy deepens, there is a significant shift from traditional anatomy toward imaging-based anatomy, particularly exemplified by the advancements in 3-D CTBA. This transition enables a more accurate understanding of bronchovascular anatomy in clinical practice.

A comparison with Li *et al.* (10) B^3 patterns is presented in *Table 1*. We reported a novel bifurcation type of the B^3 bronchus, specifically the B^3ai and $B^3aii+b+c$. We also identified a variety of arterial classifications at the sub-subsegmental level for the A^3 artery, encompassing 38 distinct types, with 27 variations specifically for A^3a. These arteries are categorised based on their branching origins, grouping into 13 unique combinations of sub-types. Following the five-type central vein model by Wang *et al.* (12) in *Table 4*, we uncovered a rare anatomical variation beyond these five classifications, namely the non-central O type.

Our detailed classifications of bronchial, arterial, and venous patterns at the LS^3 sub-subsegment level present a comprehensive framework that enhances knowledge of LUL anatomy for surgeons. Onuki and colleagues (13) proposed that lung segments do not persistently exist as distinct units from the embryonic period and that these segments are artificially named. Throughout our research, we encountered numerous confusion regarding the nomenclature of pulmonary subsegments and their ramus. If two similar three-dimensional reconstruction models exhibited subtle variations in their superior-inferior, anterior-posterior or lateral-internal relationships, it may lead to entirely different names. Our new A^3 and A^3a pulmonary arterial classification method, based on branching number, presence or absence of IL artery, and anomalous branching origins, better reflects clinical applicability and is not influenced by the pulmonary nomenclature systems. However, the efficacy and clinical feasibility of these classifications require further validation through prospective studies.

The interrelationship between pulmonary arterial, bronchial, and pulmonary venous patterns has not been well documented. Isaka *et al.* (14) were the first to identify the relationship among pulmonary artery, pulmonary vein, and bronchus patterns in LUL. Their findings are consistent with our results; however, we specifically demonstrate the correlation between the A^3a arterial branching types and the patterns of left upper division bronchi or veins. No other significant results were found among other S^3 bronchovascular patterns. This phenomenon suggests that A^3a is crucial in forming the left upper division.

The resection of pulmonary arteries and bronchi is essential for segmentectomy and subsegmentectomy, as it directly determines the extent of lung tissue excised. Previous studies (15-17) have reported that pulmonary veins in the target segment region should be divided, and the intersegmental veins should be preserved. This preservation serves as a boundary indicator of lung segments and subsegments, enhancing the precision of excisions.

The concept of three-dimensional guided, nodule-centered, and cone-shaped precise segmentectomy or combined subsegmentectomy has gained widespread recognition among thoracic surgeons. This approach has demonstrated satisfactory therapeutic outcomes and safety margins compared to lobectomy for pulmonary nodules in the middle-lateral region (18-20).

Wedge resection, the simplest form of pulmonary surgery, relies significantly on the accurate localisation of the tumour. The watershed analysis method (5), a contemporary approach to wedge resection, utilises three-dimensional reconstructions to identify target arteries. This method temporarily uses the colored ribbon to ligate the target artery with a slipknot and then administers indocyanine green for fluorescence visualisation. This approach more accurately delineates the resection

boundaries while minimizing damage associated with invasive localisation techniques, resembling the anatomical wedge resection. However, the value of IL A^3a in this study has been underestimated.

For complex nodules located between multiple lung segments or subsegments, combined resection techniques can efficiently preserve more functional lung tissue. Hong *et al.* (6) reported a new method, "Split", combined subsegmentectomy for two cases of S^3 combined with $S^{1+2}c$ and one case of S^3+$S^{1+2}c$+$S^{1+2}a$+bi. However, these procedures pose higher technical challenges and risks, leading thoracic surgeons to opt for lobectomy or broader wedge resections.

To address lung nodules in the complex region S^3a, we developed a decision tree based on various surgical approaches and anatomical insights regarding the distribution of the LS^3 pulmonary arteries and bronchi. This approach adheres to the principle of "nodule-centered, cone-shaped precise sub-lobar resection". Our innovative framework incorporates the type of pulmonary arteries and bronchi and the location of the nodules using preoperative 3-D CTBA models, offering tailored surgical recommendations. By employing this theory, we can offer optimal surgical plans for patients based on their anatomical characteristics. This tailored strategy optimizes surgical options for different patients, providing feasible alternatives for those requiring simplified surgical procedures, and equips thoracic surgeons with critical anatomical knowledge. Furthermore, it aids in anticipating the complexity of the surgical procedure, thereby fostering additional preparedness and confidence among the surgical team. For instance, if a preoperative reconstruction reveals an IL A^3a, the watershed analysis may be selected to minimise operative time and trauma. Conversely, anatomical variations such as a descending B^3a in conjunction with IL A^3a may favour a complete trans-fissure approach operation to avoid excessive damage to the anterior mediastinum.

However, this study has several potential limitations. First, the study relies solely on a fully automated noncontrast CT reconstruction algorithm (3), which may not achieve 100% accuracy and have bias between our results and real anatomical patterns. Second, the authors independently determined subsegment and sub-subsegment naming, which could be improved by more explicit procedures in future studies. Lastly, the findings of this study should be validated through multiracial research involving a larger patient cohort.

Conclusions

We identified a sub-subsegmental level within the left S^3 bronchovascular distribution patterns and defined the frequency of anatomic variations in 635 patients using 3-D CTBA. This study also confirmed the correlation between A^3a with B^3, A^3, and LUDV. The abnormal A^3a, which originates from the IL portion of LPA, is common, having a frequency rate of 16.06% (102/635) among people. For surgeons intending to perform subsegmentectomies, the five ectopic origins of LA, IL LPA, IL $A^{1+2}c$, MLA, and $A^{1+2}a$+b are crucial for locating the A^3a. Meanwhile, for those opting to select a concise wedge resection, the watershed analysis method and the occurrence of IL A^3a can make the operation easier.

Acknowledgments

None.

Footnote

Reporting Checklist: The authors have completed the STROBE reporting checklist. Available at https://jtd.amegroups.com/article/view/10.21037/jtd-24-1397/rc

Data Sharing Statement: Available at https://jtd.amegroups.com/article/view/10.21037/jtd-24-1397/dss

Peer Review File: Available at https://jtd.amegroups.com/article/view/10.21037/jtd-24-1397/prf

Funding: This work was supported by the Affiliated People's Hospital of Jiangsu University (No. Y2022023) and the Key Project of Jiangsu Commission of Health (No. ZD2022055).

Conflicts of Interest: All authors have completed the ICMJE uniform disclosure form (available at https://jtd.amegroups.com/article/view/10.21037/jtd-24-1397/coif). The authors have no conflicts of interest to declare.

Ethical Statement: The authors are accountable for all aspects of the work in ensuring that questions related to the accuracy or integrity of any part of the work are appropriately investigated and resolved. The study was conducted in accordance with the Declaration of Helsinki (as revised in 2013). The study was approved by the Ethics Committee of Affiliated People's Hospital of Jiangsu

University (No. SQK-20220166-Y) and individual consent for this retrospective analysis was waived.

References

1. Saji H, Okada M, Tsuboi M, et al. Segmentectomy versus lobectomy in small-sized peripheral non-small-cell lung cancer (JCOG0802/WJOG4607L): a multicentre, open-label, phase 3, randomised, controlled, non-inferiority trial. Lancet 2022;399:1607-17.
2. Altorki N, Wang X, Kozono D, et al. Lobar or Sublobar Resection for Peripheral Stage IA Non-Small-Cell Lung Cancer. N Engl J Med 2023;388:489-98.
3. Chen X, Wang Z, Qi Q, et al. A fully automated noncontrast CT 3-D reconstruction algorithm enabled accurate anatomical demonstration for lung segmentectomy. Thorac Cancer 2022;13:795-803.
4. Decaluwe H, Petersen RH, Hansen H, et al. Major intraoperative complications during video-assisted thoracoscopic anatomical lung resections: an intention-to-treat analysis. Eur J Cardiothorac Surg 2015;48:588-98; discussion 599.
5. Chu XP, Chen ZH, Lin SM, et al. Watershed analysis of the target pulmonary artery for real-time localization of non-palpable pulmonary nodules. Transl Lung Cancer Res 2021;10:1711-9.
6. Hong R, Chen C, Zheng W, et al. "Split" combined subsegmentectomy: A case series. Thorac Cancer 2022;13:423-9.
7. Boyden EA. Segmental anatomy of the lungs a study of the patterns of the segmental bronchi and related pulmonary vessels. New York: McGraw-Hill; 1955:185-200.
8. Yamashita HJ. Roentgenologic Anatomy of the Lung. Stuttgart: Georg Thieme Publishers; 1978.
9. Chen L, Zhu Q, Wu W. Atlas of thoracoscopic anatomi pulmonary subsegmentectomy. Amsterdam: Elsevier; 2023.
10. Li Z, Zhao Q, Wu W, et al. Analysis of bronchovascular patterns in the left superior division segment to explore the relationship between the descending bronchus and the artery crossing intersegmental planes. Front Oncol 2023;13:1183227.
11. Chassagnon G, Morel B, Carpentier E, et al. Tracheobronchial Branching Abnormalities: Lobe-based Classification Scheme. Radiographics 2016;36:358-73.
12. Wang J, Lin H, Bian C, et al. A modified system for classifying the bilateral superior pulmonary veins using three-dimensional computed tomography bronchography and angiography images. J Thorac Dis 2021;13:5933-41.
13. Onuki T, Kanzaki M, Wachi N, et al. Do the lung segments exist continuously from the early stage of the embryonic period as units? Interact Cardiovasc Thorac Surg 2016;23:26-30.
14. Isaka T, Mitsuboshi S, Maeda H, et al. Anatomical analysis of the left upper lobe of lung on three-dimensional images with focusing the branching pattern of the subsegmental veins. J Cardiothorac Surg 2020;15:273.
15. Oizumi H, Endoh M, Takeda S, et al. Anatomical lung segmentectomy simulated by computed tomographic angiography. Ann Thorac Surg 2010;90:1382-3.
16. Oizumi H, Kanauchi N, Kato H, et al. Anatomic thoracoscopic pulmonary segmentectomy under 3-dimensional multidetector computed tomography simulation: a report of 52 consecutive cases. J Thorac Cardiovasc Surg 2011;141:678-82.
17. Wu WB, Xu XF, Wen W, et al. Three-dimensional computed tomography bronchography and angiography in the preoperative evaluation of thoracoscopic segmentectomy and subsegmentectomy. J Thorac Dis 2016;8:S710-5.
18. Li Z, Xu W, Pan X, et al. Segmentectomy versus lobectomy for small-sized pure solid non-small cell lung cancer. Thorac Cancer 2023;14:1021-8. Erratum in: Thorac Cancer 2024;15:1038.
19. Li Z, Xu W, Wang J, et al. Three-Dimensional Guided Cone-Shaped Segmentectomy Versus Lobectomy for Small-sized Non-Small Cell Lung Cancer in the Middle Third of the Lung Field. Ann Surg Oncol 2023;30:6684-92.
20. Wu WB, Xia Y, Pan XL, et al. Three-dimensional navigation-guided thoracoscopic combined subsegmentectomy for intersegmental pulmonary nodules. Thorac Cancer 2019;10:41-6.

Cite this article as: Long T, Qi J, Shao A, Zhu J, Pan H, Shi Y, Ren Z, He Z, Wu W. Analysis of left anterior segmental bronchovascular patterns and its benefits for surgical implications: a retrospective cross-sectional study. J Thorac Dis 2025;17(1):174-186. doi: 10.21037/jtd-24-1397